The International Journal of Advanced Manufacturing Technology (2018) 98:1367–1377
https://doi.org/10.1007/s00170-018-2125-4

ORIGINAL ARTICLE

Force predictive model for five-axis ball end milling of sculptured surface

Z. C. Wei[1] · M. L. Guo[1] · M. J. Wang[1] · S. Q. Li[1] · S. X. Liu[1]

Received: 15 November 2017 / Accepted: 6 May 2018 / Published online: 19 June 2018

Abstract
As a high precision and high efficiency cutting method, CNC milling of five axis is the first choice for manufacturing parts with complex sculptured surface. Milling force is one of the most important physical parameters in machining which affects the cutting vibration, cutting deformation, cutting heat, and surface quality directly. Aiming at the five-axis ball end milling of sculptured surface, a force predictive model with arbitrary cutter axis vector and feed direction is established. The conditions of micro-cutting edge of three-axis ball end mill involved in cutting are determined by space region limitation at the first. Then, after space rotation transformation, an analytic in-cut cutting edge (ICCE) method for five-axis ball end milling of oblique plane is proposed by judging micro-cutting edge one by one. Based on the idea of differential discretization, the machining of general complex surface can be regarded as a combination of a series of tiny oblique planes. Drawing on the idea to sculptured surface and combining micro-element milling force model and undeformed chip thickness model that is suitable for five-axis ball end milling with arbitrary feed direction, a milling force predictive model for five-axis ball end milling of sculptured surface is established. The results of simulations and experiments show that the ICCE determined by the space region limitation is consistent with the traditional Z-map method and the solid modeling method with high efficiency and precision. The measured force and the predictive force of the five-axis milling on sculptured surface are in good agreement in amplitude and trend, which proves the effectiveness of the milling force predictive model of five-axis ball end milling of sculptured surface.

Keywords ICCE · Sculptured surface · Five-axis machining · Ball end mill · Prediction of milling force

1 Introduction

Large complex surface parts such as propeller, mechanical impeller, and automotive cover precision mold have a wide range of applications in the aerospace, automobile, mold, energy, and other major equipment manufacturing territory. Ball end mill has the characteristics of shape self-adaptability and simple programming. It has been widely used in the machining of complex sculptured surface parts. Milling force directly affects the cutting vibration, cutting deformation, cutting heat, and surface quality, and it is the important basis of calculating the cutting power, optimizing the process parameters, and designing machine tools, cutters, and fixtures. In five-axis ball end milling, the surface geometry of the workpiece is complicated. The cutter axis vector and the tool path change arbitrarily, so the number of teeth and the in-cut cutting edge (ICCE) of teeth involved in cutting change at each different cutter location point. ICCE, the core of the prediction of milling force, defines the valid range of undeformed chip thickness model.

In the 1940s, Martellotti et al. [1] studied the kinematic characteristics of the milling process and proposed a mathematical expression of the undeformed chip thickness, which is the basis for the analysis and establishment of the milling force predictive model. Subsequently, the study of the prediction of the milling force had been mainly aimed at the non-ball end mill [2–4] until South Korea's Yang et al. [5] published the first study of ball end mill in 1991. Since that, scholars have been made fruitful research results in milling force modeling and forecasting for the ball mill steady milling. Yucesan et al. [6] and Wang et al. [7] have established the milling force predictive model for the three-axis horizontal machining of the ball end mill. For three-axis complex surface

✉ Z. C. Wei
wei_zhaocheng@dlut.edu.cn

[1] Key Laboratory for Precision and Non-traditional Machining Technology of Ministry of Education, Dalian University of Technology, Dalian 116024, China

machining, the difficulties are the definition of the instantaneous undeformed chip and the ICCE. Tsai et al. [8] and Azeem et al. [9] have studied the instantaneous undeformed chip thickness in different feed directions and tool paths. Imani et al. [10] extracted the cutter workpiece engagement boundary based on the ACIS geometry kernel and expressed it with the B-spline curve. The ICCE, obtained by calculating the intersection points of cutter workpiece engagement boundary curve and cutter edge, was used to establish the milling force model. The Z-map method based on discrete thinking rays line from points projected in a plane to cutter and workpiece along given direction (usually *Z*-axis) and determines the cutter workpiece engagement by comparing the coordinate of *z*. After that, the ICCE was obtained by finding the intersection points of cutting edge and cutter workpiece engagement boundary curve [11–14]. Fontaine et al. [15] proposed conditions of micro-cutting edge involved in cutting and established milling force model for the ball end milling of 2.5-dimensional wavelike form surface, and it has application limitation when cutting environment changes.

With the continuous development of multi-axis CNC equipment, the application of five-axis ball end milling has become an inevitable trend. The cutter axis vector of five-axis ball end milling relative to workpiece varies arbitrarily. So, the models of instantaneous undeformed chip thickness and ICCE in three-axis milling need to be redefined and they are more difficult to solve. On the other hand, the processing condition at each cutter location point is different, which results in a large amount of milling force simulation of the whole cutting process. Ozturk et al. [16] took the range of simple axial position angle as window function to define ICCE and put forward a five-axis slotting milling with ball end mill. Then, they discussed the cutter contact information of ball end mill in large axial cutting machining with different combinations of processing parameters and established five-axis non-slotting milling force predictive model [17]. Generally, based on solid modeling method [18, 19] and discretization method [20–22], cutter workpiece engagement is obtained at the first. Then, the relative position of the cutting edge and cutter workpiece engagement is analyzed, finally extracting the ICCE. This process is also suitable for five-axis machining, but there is often a tradeoff between efficiency and accuracy. With three-axis ball end milling being study object, Wang et al. [23] and Geng et al. [24] discretized the depth of cut along the direction of cutter axis, then obtained cut-in and cut-out angles based on each thin layer, furthermore got the cutter workpiece engagement of five-axis milling through coordinate rotation transformation. Sun et al. [25] back computed ICCE by combining the known unprocessed surface and the final processing surface with the instantaneous chip thickness of micro-cutting edge. In the five-axis ball end milling, the thickness of the instantaneous undeformed chip is defined by the projection vector of the feed in the norm of micro-cutting edge [17, 21, 23, 24], or the distance of removed material measured along the connection line of micro-cutting edge and the center of sphere [20, 22, 25]. Huang et al. [26] studied the influence of lead and tilt angles on the thickness of the undeformed chip thickness. Although the above-mentioned literatures have achieved the five-axis milling force prediction of ball end mill, the ICCE is complicated to solve. Because efficiency and accuracy cannot combine at the same time, it is difficult to apply the five-axis ball end milling to large and complex surface.

In this paper, an analytical ICCE algorithm based on space region limitation for five-axis ball end milling of complex sculptured surface is proposed. Then, a milling force predictive model of five-axis ball end milling on sculptured surface is established. General idea is shown as Fig. 1. Three-axis ball end milling as the object of study, the conditions of micro-cutting edge involved in cutting are determined by space region limitation. Based on the space rotation transformation, the whole cutting edge will be searched and judged, and the analytical ICCE algorithm suitable for five-axis ball end milling of oblique plane is obtained. Based on the idea of differential discretization, the surface machining is discretized into a series of oblique plane machining and the discretized density can be set by the cutting step. Then, the analytical ICCE algorithm for the five-axis ball end milling of sculptured surface is obtained. Combined with the undeformed chip thickness model and the micro-milling force model suitable for five-axis ball end milling of sculptured surface, the five-axis milling force prediction model for the ball end milling of sculptured surface is established.

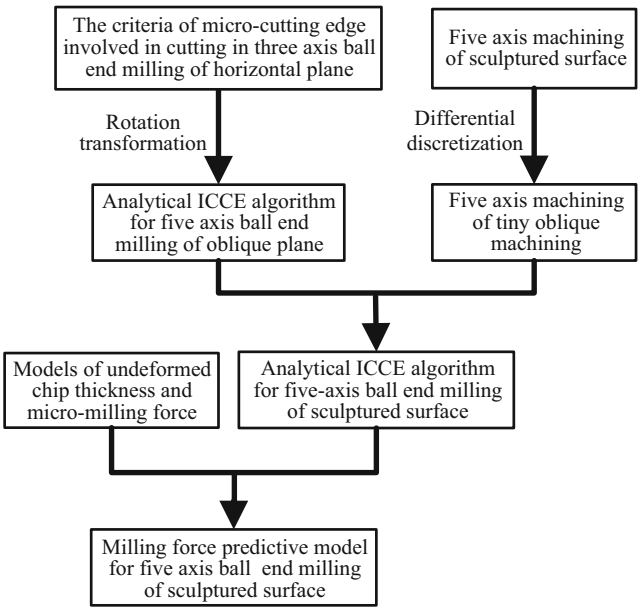

Fig. 1 General idea

2 Analytical algorithm of ICCE

Based on differential discretization, sculptured surface can be discretized into a series of oblique planes. Based on space rotation transformation, five-axis machining of oblique plane can be converted to the corresponding three-axis machining. Taking three-axis milling of horizontal plane as study object, the conditions that micro-cutting edge participates in cutting can be proposed easily.

It shows that the five-axis machining of oblique plane with arbitrary feed direction and cutter axis vector in Fig. 2. In order to facilitate the establishment of the milling force predictive model, the spherical center of cutter is defined as the origin of the cutter coordinate system. The cutter axis vector $\boldsymbol{p}$ is the O-Z_c axis of cutter coordinate system. The O-X_c axis is the cross product of $\boldsymbol{p}$ and normal vector of oblique plane $\boldsymbol{n}$. O-Y_c axis is obtained from the right-hand coordinate system. The programming coordinate system is defined as the static workpiece coordinate system O-$X_wY_wZ_w$. The inclination angle ε is defined as the angle between the normal vector of oblique plane $\boldsymbol{n}$ and cutter axis vector $\boldsymbol{p}$. The feed direction angle γ is the angle between O-X_c and feed direction $\boldsymbol{f}$. When $(\boldsymbol{p}\times\boldsymbol{n})\times\boldsymbol{f}$ points to the negative direction of the $\boldsymbol{n}$, the feed direction angle γ is positive; otherwise, γ is negative. When $\boldsymbol{p}\times\boldsymbol{n}$ points to the negative direction of the $\boldsymbol{n}$, the inclination angle ε is positive; otherwise, ε is negative. The expressions are as follows:

$$\varepsilon = \arccos\left(\frac{\mathbf{n}\cdot\mathbf{p}}{|\mathbf{n}||\mathbf{p}|}\right) \tag{1}$$

$$\gamma = \arccos\left(\frac{(\mathbf{p}\times\mathbf{n})\cdot\mathbf{f}}{|\mathbf{p}\times\mathbf{n}||\mathbf{f}|}\right) \tag{2}$$

2.1 Cutting edge of ball end mill

The shape of the cutting edge of the ball end mill is complicated generally. In addition to simple tipped ball end mill, ball end mill with constant lead spherical helix cutting edge is widely used, which is the projection of flat end mill with constant helix angle on sphere. In the same direction of the rotation direction of the cutter, this paper uses the clockwise direction as the positive direction of the horizontal angle measurement. The typical constant lead spherical helix is shown in Fig. 3.

The micro-cutting edge on the cutting edge is monotonically corresponding to the axial position angle k measured from the negative direction of the O-Z_c axis. Axial position angle of micro-cutting edge taken as the parameter, the expression of the arbitrary point on the spherical helix cutting edge in cutter coordinate is as follows:

$$\begin{cases} X_j = R\sin k\sin\theta \\ Y_j = R\sin k\cos\theta \\ Z_j = -R\cos k \\ \theta = \psi_j - \varphi(k) \\ \psi_j = \psi - (j-1)2\pi/m \end{cases} \tag{3}$$

where

$$\varphi(k) = \frac{(R - R\cos k)\tan\alpha}{R} \tag{4}$$

In the formula, R is the radius of cutter. ψ is the radial location angle of the cutting edge and θ is the radial location angle of the micro-cutting edge. They represent the

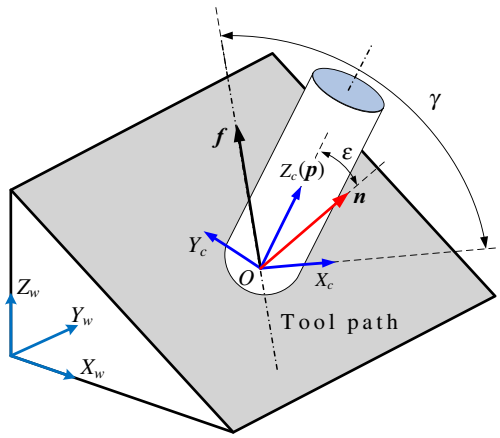

Fig. 2 Five-axis ball end milling of oblique plane

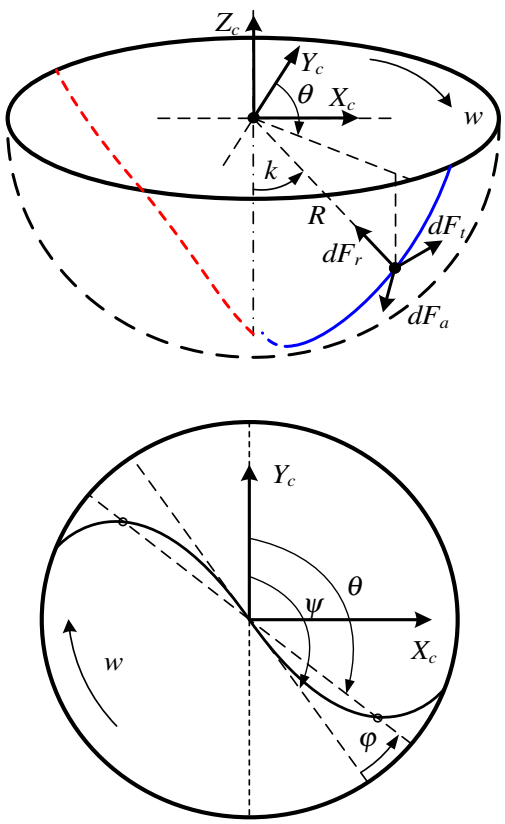

Fig. 3 Constant lead helix cutting edge for ball end mill

position of the cutting edge and micro-cutting edge relative to the O-Y_c axis. φ is helix lag angle of the micro-cutting edge relative to the cutting edge. α is the helical angle of the ball end mill. They are measured deasil. m is the number of cutter teeth.

2.2 Criteria of micro-cutting edge involved in cutting for five-axis milling

Study the simple relatively three-axis ball end milling of horizontal plane at first. As shown in Fig. 4, *aa* represents cylindrical surface swept by former tool path; *bb* is the plane through the center of cutter and perpendicular to the feed direction. *cc* is both the upper surface of workpiece and the machining allowance surface at the same time.

Assuming that a point $P(x_0, y_0, z_0)$ on cutting edge is located in cutter workpiece engagement, then the following three conditions must be met:

1) The point P is located outside the cylindrical space *aa*, the condition can be expressed as a mathematical formula:

$$(y_0 - s)^2 + {z_0}^2 > R^2 \tag{5}$$

where s is step distance.

2) The point P is located on the feed direction side of the plane *bb*, which can be expressed as a mathematical expression:

$$x_0 > 0 \tag{6}$$

3) The point P is under the machining-allowance surface *cc*, which can be expressed as a mathematical formula:

$$R + z_0 < d_n \tag{7}$$

For general five-axis machining of oblique plane, the micro-cutting edge should be transformed into three-axis milling of horizontal plane through space rotation transformation and then judged whether it satisfies the above three conditions. For example, a point $P(x_0, y_0, z_0)$ is on cutting edge which is corresponding to point $Q(x_1, y_1, z_1)$ in three-axis milling of horizontal plane through reverse rotation transformation.

$$[x_1 \;\; y_1 \;\; z_1] = [x_0 \quad y_0 \quad z_0] \cdot T_{x(\varepsilon)} \cdot T_{z(\gamma)} \tag{8}$$

Rotation matrix $T_{\boldsymbol{x}(\varepsilon)}$ represents that the rotation axis is $\boldsymbol{x}$ and the rotation angle is the slope inclination angle ε. $T_{\boldsymbol{z}(\gamma)}$ represents rotation matrix about $\boldsymbol{z}$ and the rotation angle is feed direction angle γ. $\boldsymbol{x}$ is the vector of O-X_c axis in cutter coordinate system, that is, [1 0 0]. $\boldsymbol{z}$ is the vector of O-Z_c axis in cutter coordinate system obtained from the first rotation, that is, [0 0 1]. Take $T_{\mathbf{x}(\varepsilon)}$ as an example, the expression is:

$$\begin{aligned} \mathrm{x} &= (\mathrm{x}_x \quad \mathrm{x}_y \quad \mathrm{x}_z) \\ \mathbf{T}_{\mathrm{x}(\varepsilon)} &= \begin{bmatrix} \mathrm{x}_x{}^2 + (1 - \mathrm{x}_x{}^2)\cos\varepsilon & \mathrm{x}_x\mathrm{x}_y(1-\cos\varepsilon) + \mathrm{x}_z\sin\varepsilon & \mathrm{x}_x\mathrm{x}_z(1-\cos\varepsilon) - \mathrm{x}_y\sin\varepsilon \\ \mathrm{x}_x\mathrm{x}_y(1-\cos\varepsilon) - \mathrm{x}_z\sin\varepsilon & \mathrm{x}_y{}^2 + (1-q_y{}^2)\cos\varepsilon & \mathrm{x}_y\mathrm{x}_z(1-\cos\varepsilon) + \mathrm{x}_x\sin\varepsilon \\ \mathrm{x}_x\mathrm{x}_z(1-\cos\varepsilon) + \mathrm{x}_y\sin\varepsilon & \mathrm{x}_y\mathrm{x}_z(1-\cos\varepsilon) - \mathrm{x}_x\sin\varepsilon & \mathrm{x}_z{}^2 + (1-\mathrm{x}_z{}^2)\cos\varepsilon \end{bmatrix} \end{aligned} \tag{9}$$

For ball end five-axis milling of oblique plane, to determine whether the point P is located in the cutter workpiece engagement, it is necessary to determine whether the corresponding point Q is located in the cutter workpiece engagement of three-axis milling. If the point Q meets the three conditions mentioned above, the point P is involved in cutting; otherwise, the point P is not involved in cutting.

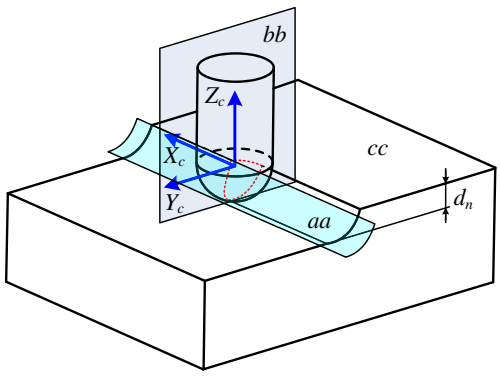

Fig. 4 Three-axis down milling of horizontal plane with ball end mill

2.3 Algorithm flow of ICCE in five-axis milling

During the cutting process, a part of cutting edge is involved in cutting. The cutting edge between two end points is used to indicate the cutting edge that is actually involved in the milling, that is, the ICCE. Since this paper uses axial position angle k to represent micro-cutting edge, the ICCE is expressed as an array $[k_{\mathrm{low}}, k_{\mathrm{up}}]$ as shown in Fig. 5.

Based on the above criteria, the micro-cutting edge is judged one by one. Two micro-cutting edges can be found near any boundary points of ICCE that one is involved in cutting and the other is not involved in cutting.

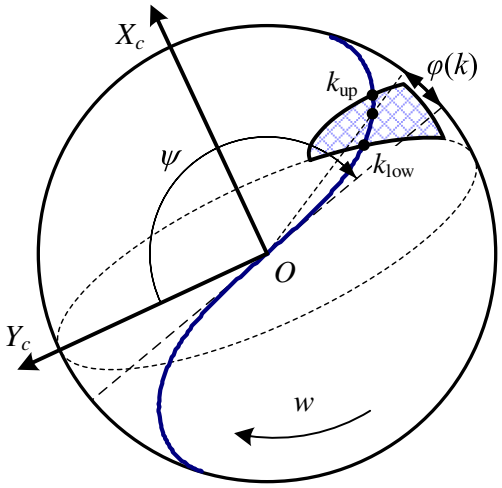

Fig. 5 ICCE of ball end mill

Dichotomous search method will be used to search for precise ICCE further. The ICCE algorithm flowchart is shown in Fig. 6. The algorithm can obtain ICCE of a cutting edge during a cutter revolution. To get the ICCE of the other cutter edge, it just only increases the phase of the previous cutter edge by one tooth pitch angle $2\pi/m$.

3 Milling force model

With five-axis ball end milling of oblique plane as studied object, this paper adopts Armarego's mechanical linear micro-cutting edge force model, which separates cutting

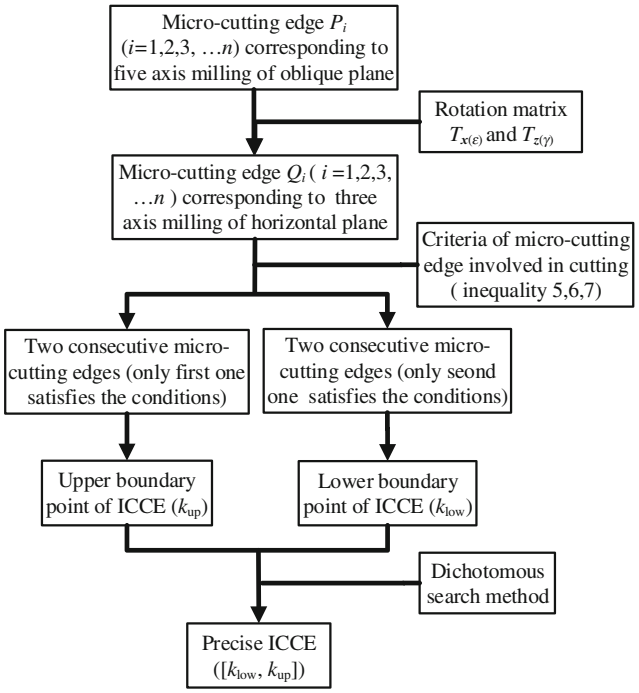

Fig. 6 Flowchart of calculating ICCE

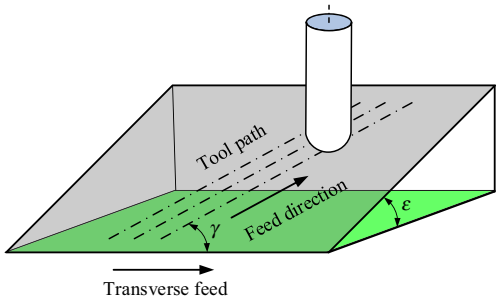

Fig. 7 ICCE simulation of three-axis machining on oblique plane

force into shear force and plowing force in milling. The force of micro-element on cutting edge j is expressed as:

$$\begin{cases} dF_{r,j} = K_{re}dS + K_{rc}t_n db \\ dF_{t,j} = K_{te}dS + K_{tc}t_n db \\ dF_{a,\mathrm{j}} = K_{ae}dS + K_{ac}t_n db \end{cases} \tag{10}$$

where dF_r, dF_t, and dF_a are the radial, tangential, and axial force of the micro-cutting edge respectively. K_{re}, K_{te}, and K_{ae} are the radial, tangential, and axial plowing force coefficients of the micro-cutting edge, respectively. K_{rc}, K_{tc}, and K_{ac} are the radial, tangential, and axial shear force coefficients of the micro-cutting edge respectively. The dS is the length of the micro-cutting edge involved in cutting; db is the width of the micro-chip.

The formula of the width of micro-chip is:

$$db = R{\cdot}dk \tag{11}$$

From Formula (3), the cutting edge's vector expression of ball end mill with constant lead is:

$$\mathbf{r}(k) = R\sin k\sin\left(\psi_j - \varphi(k)\right)\mathbf{i} + R\sin k\cos\left(\psi_j - \varphi(k)\right)\mathbf{j} + (R - R\cos k)\mathbf{k} \tag{12}$$

The length of micro-edge dS is expressed as:

$$dS = R\sqrt{1 + \sin^4 k\tan^2\alpha}{\cdot}dk \tag{13}$$

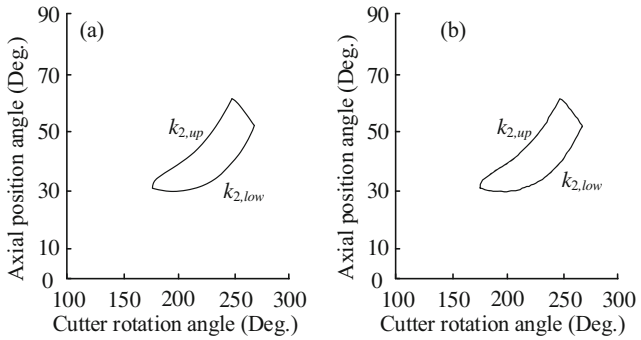

Fig. 8 Simulation results of ICCE. **a** Analytical algorithm. **b** Z-map model

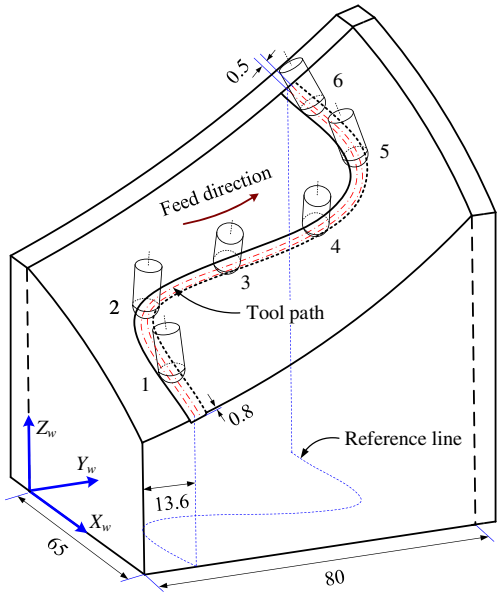

Fig. 9 ICCE simulation of five-axis machining on surface

The change of feed direction influences thickness of undeformed chip in five-axis ball end milling. Hence, this paper defines undeformed chip thickness as the projection of the feed vector in the direction of the cutter's sphere normal vector according to the study of Merdol. The feed vector $\boldsymbol{f}$ and the cutter's spherical normal vector $\boldsymbol{n}$ are calculated as:

$$\begin{cases} \boldsymbol{f} = f_c \cdot \boldsymbol{f}_u = f_c \cos\gamma \cdot \boldsymbol{i} + f_c \cos\eta \cdot \boldsymbol{j} + f_c \cos\xi \cdot \boldsymbol{k} \\ \boldsymbol{n} = \sin k \sin\theta \cdot \boldsymbol{i} + \sin k \cos\theta \cdot \boldsymbol{j} - \cos k \cdot \boldsymbol{k} \end{cases} \tag{14}$$

$$\eta = \arccos\left(\frac{(\mathbf{p} \times (\mathbf{p} \times \mathbf{n})) \cdot \mathbf{f}}{|(\mathbf{p} \times (\mathbf{p} \times \mathbf{n}))||\mathbf{f}|}\right) \tag{15}$$

$$\xi = \arccos\left(\frac{\mathbf{p} \cdot \mathbf{f}}{|\mathbf{p}||\mathbf{f}|}\right) \tag{16}$$

where $\boldsymbol{f_c}$ is the feed per tooth and $\boldsymbol{f_u}$ is the unit vector in feed direction. Vectors $\boldsymbol{i}$, $\boldsymbol{j}$, and $\boldsymbol{k}$ are the unit vectors of positive directions of X_c-axis, Y_c-axis, and Z_c-axis respectively. γ, η, and ξ are the angles between unit vector $\boldsymbol{f_u}$ and the positive directions of X_c-axis, Y_c-axis, and Z_c-axis respectively.

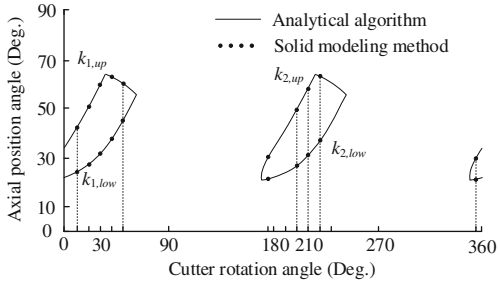

Fig. 10 Simulation results of ICCE

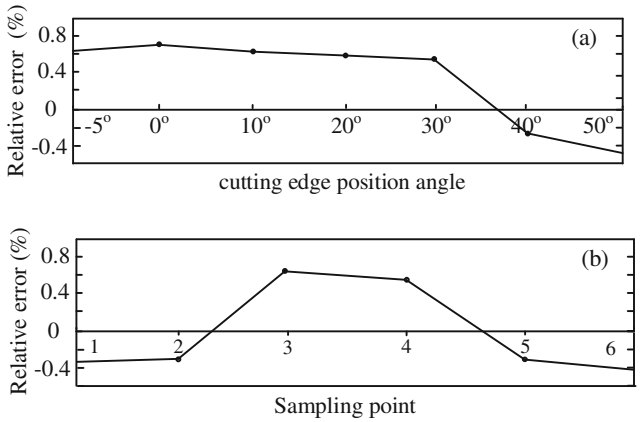

Fig. 11 **a**, **b** Simulation errors of ICCE

For the ICCE [k_{low}, k_{up}], the calculation model of undeformed chip thickness t_n corresponding to micro-cutting edge of the ball end mill is expressed as follows:

$$t_n = f_c \cos\gamma \sin k \sin\theta + f_c \cos\eta \sin k \cos\theta - f_c \cos\xi \cos k \quad (k_{\text{low}} < k < k_{\text{up}}) \tag{17}$$

The matrix transformation formula for projecting the micro-element milling forces of the jth cutter tooth into the cutter coordinate system $O\text{-}X_cY_cZ_c$ is:

$$\begin{bmatrix} dF_{x,j}(\theta(\psi,k)) \\ dF_{y,j}(\theta(\psi,k)) \\ dF_{z,j}(\theta(\psi,k)) \end{bmatrix} = \begin{bmatrix} -\cos\theta_j & -\sin k \sin\theta_j & -\cos k \sin\theta_j \\ \sin\theta_j & -\sin k \cos\theta_j & -\cos k \cos\theta_j \\ 0 & \cos k & -\sin k \end{bmatrix} \begin{bmatrix} dF_{t,j} \\ dF_{r,j} \\ dF_{a,j} \end{bmatrix} \tag{18}$$

Formulas (10), (11), (13), and (17) brought into (18); then, with micro-element milling forces integrated numerically along ICCE, the overall milling force of cutting edge j can be obtained. In order to obtain the three-direction milling forces of the cutter at any time, the forces of all cutter edges are summed up. The formula is:

$$[F_{XcYcZc}(\psi)] = \sum_{j=1}^{m} \int_{k\text{low},j}^{k\text{up},j} \left(\left[A_{e,j}^{XcYcZc} \right] + \left[A_{c,j}^{XcYcZc} \right] \right) dk \tag{19}$$

$$[F_{XcYcZc}(\psi)] = [\, F_{Xc}(\psi) \quad F_{Yc}(\psi) \quad F_{Zc}(\psi) \,]^T \tag{20}$$

Table 1 Comparison of the calculation methods of ICCE

Method	Precision	Efficiency
Solid modeling	High	Low
Z-map	Low	High
Analysis	High	High

where

$$\left[A_{e,j}^{XcYcZc}\right] = R\sqrt{1+\sin^4 k\tan^2\alpha}\begin{bmatrix} -K_{te}\cos\theta_j - K_{re}\sin k\sin\theta_j - K_{ae}\cos k\sin\theta_j \\ K_{te}\sin\theta_j - K_{re}\sin k\cos\theta_j - K_{ae}\cos k\cos\theta_j \\ K_{re}\cos k - K_{ae}\sin k \end{bmatrix} \tag{21}$$

$$\left[A_{c,j}^{XcYcZc}\right] = R(f_c\cos\gamma\sin k\sin\theta + f_c\cos\eta\sin k\cos\theta - f_c\cos\xi\cos k) \begin{bmatrix} -K_{tc}\cos\theta_j - K_{rc}\sin k\sin\theta_j - K_{ac}\cos k\sin\theta_j \\ K_{tc}\sin\theta_j - K_{rc}\sin k\cos\theta_j - K_{ac}\cos k\cos\theta_j \\ K_{rc}\cos k - K_{ac}\sin k \end{bmatrix} \tag{22}$$

Based on the idea of differential discretization, each instantaneous cutter point of five-axis machining on sculptured surface can be regarded as five-axis milling on oblique plane. The density of the cutter points can be set by the cutting step distance. The direction of line formed by two successive cutter location points is regarded as the feed direction of the previous cutter location point. Geometric information such as the normal of the workpiece at each cutter location point and the cutter axis vector is obtained from the programming software. Therefore, based on the above-mentioned milling force model for five-axis ball end milling of oblique plane, the prediction of milling force for five-axis ball end milling of sculptured surface can be achieved.

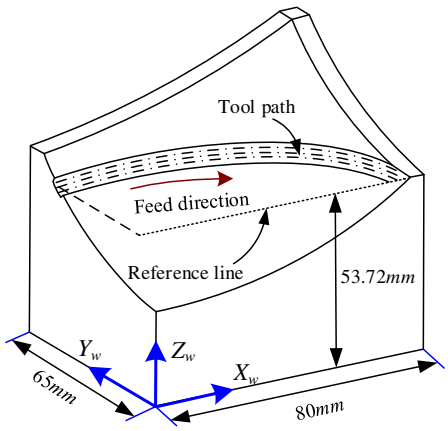

(a)

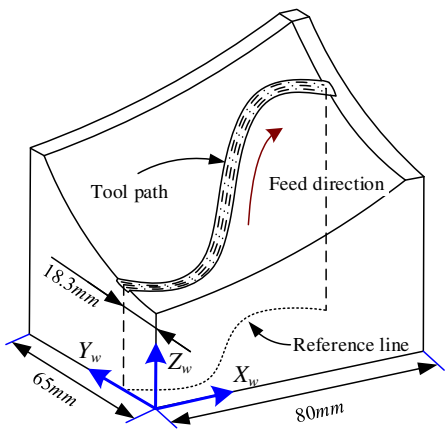

(b)

Fig. 12 Schematic diagram of workpiece. **a** Z-constant tool path milling. **b** Sinusoidal tool path milling

4 Experiments and simulations

4.1 Simulation examples for ICCE

In order to verify the validity of the algorithm for solving ICCE based on the space region limitation method, compared with Z-map model and the solid modeling method, simulation machining examples including three-axis milling on oblique plane and five-axis milling on sculptured surface are carried out.

The ICCE algorithm proposed in this paper is based on the oblique plane machining. So the first simulation condition is as follows: the diameter of ball end mill with two flutes used in down milling on oblique plane is 6 mm, and dextral helix angle is 30°; the step distance, depth of cut, inclination angle, and feed direction angle are 0.25 mm, 0.8 mm, 20°, and 75°, respectively. The detailed simulation geometry is shown in Fig. 7.

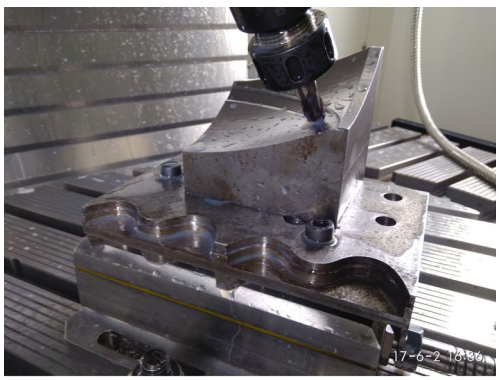

(a)

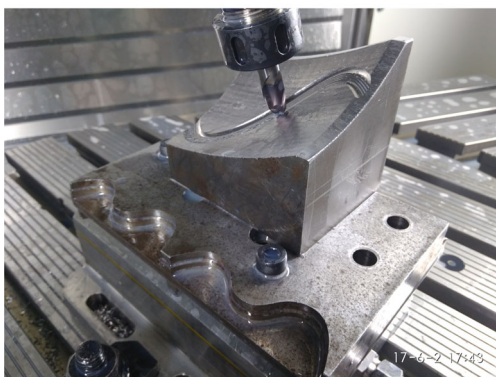

(b)

Fig. 13 Five-axis ball end milling experiments of sculptured surface. **a** Z-constant machining. **b** Sinusoidal machining

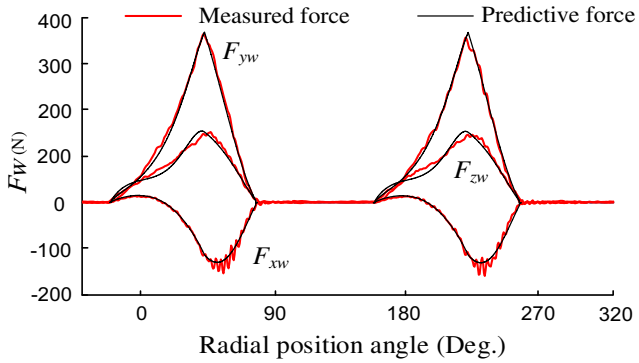

Fig. 14 Verification of cutting force coefficients

The simulation result of ICCE based on the analytical algorithm is shown in Fig. 8a, while the simulation result of the Z-map model based on the discrete principle proposed by Wei et al. [13] is shown in Fig. 8b, in which the upper and lower bound curves of ICCE are not smooth. The main reason is that there exists a grid round error in calculation process, which leads to the curve unsmooth. As a contrast, the Fig. 8a curve is based on the analytical algorithm and obtained by dichotomous search method, so the calculation error is very small and the curve is smooth. The results show that if the influence of roundness error is neglected, the results of the two simulations are almost identical, which prove the validity of the analytical algorithm. In addition, compared with the Z-map model method, the analytical algorithm does not require a lot of data storage; thus, it has high computational efficiency.

It is generally believed that the precision of the ICCE solved by Unigraphics NX based on solid modeling is high. In order to explore the accuracy of the analytical ICCE algorithm proposed in this paper, the following simulation example is arranged. The analytical equation of the surface is: $0.01x^{1.8} - 0.008y^{1.9} - 1.5z + 2.3 = 0$ $(0 \le x \le 65,\ 0 \le y \le 80)$. The tool path is projected from the sinusoidal curve whose expression is $y = 18\sin(2\pi x)$ $(0 \le x \le 1)$ and extends naturally to the boundary. The cutter is the same as described in the above three-axis simulation experiment. The front lean angle and roll angle of cutter axis vector relative to part geometry are 20° and 10° respectively. Other relevant parameters are shown in Fig. 9.

Six points are sampled equally along the tool path. According to the idea of differential discretization, the corresponding five-axis machining model of oblique plane is set up at each cutter location point. The tangent plane of the surface at the sampling point is an oblique plane whose normal direction is the normal direction of sculptured surface. The feed direction of oblique plane milling is the

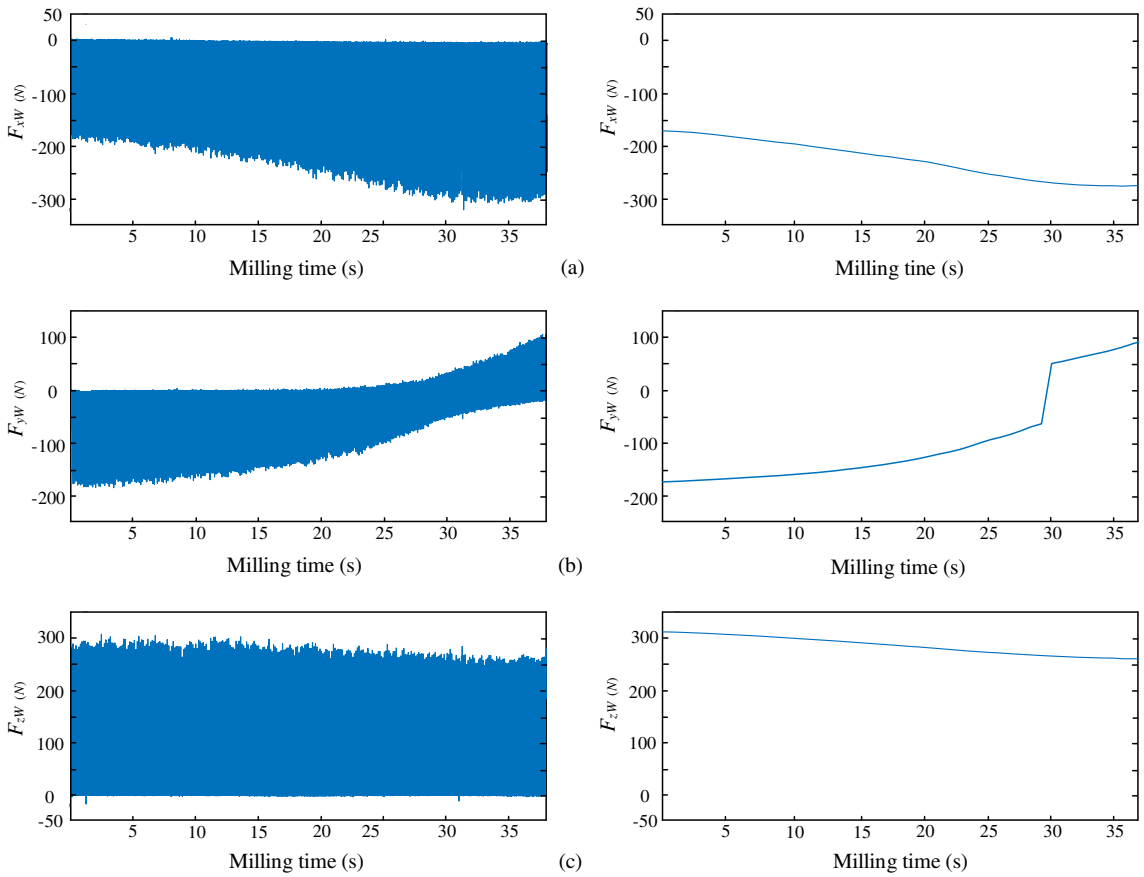

Fig. 15 **a**–**c** Three-direction milling forces predictive results of Z-constant tool path

tangent line of tool path at sampling point. Based on this, when cutter makes one revolution, the ICCE of the two cutting edges at arbitrary cutting edge position angle at the first sampling point is obtained. The result based on the analytical algorithm presented in this paper is shown as solid line in Fig. 10, while the ICCE, based on the Unigraphics NX modeling module and its analysis and measurement tool, is obtained at the cutting edge position angles of −5°, 0°, 10°, 20°, 30°, 40°, and 50°, as the points shown in Fig. 10. Supposing that the ICCE obtained from solid modeling method is accurate absolutely, the error results of axial position angle k of the upper and lower boundary points at the seven instantaneous position angles are shown as dotted line in Fig. 11a, and the error results corresponding to the six sampling points are shown as solid line in Fig. 11b at the cutting edge position angle of 45°. The curvature of the surface at cutter location point, the curvature of tool path, and the surface formed by the different tool paths all have an influence on the analytical algorithm that is based on the oblique plane machining, so there will be some deviations and the errors are less than 1%. Furthermore, the precision of ICCE can be improved by increasing the discrete number of cutting edge position angle and axial position angle, as well as improving precision of dichotomous search. The simulation results show the effectiveness of the analytical ICCE algorithm in surface machining.

Solid modeling method has high precision, but the efficiency is low. The simulation example is done on a personal computer that is configured as: Processor Intel (R) Core (TM) i5-4590 CPU 3.30 GHz, install memory (RAM) 4.00 GB. For a cutter with two flutes making a revolution, the mean simulation time of ICCE at six cutter location points is 0.083640 s. It shows that the algorithm has obvious advantage over the solid modeling method.

To sum up, comparing the solid modeling method and Z-map method, the ICCE analytical method proposed in this paper has the advantages of efficiency and precision at the same time. It is more suitable for large complex surface machining simulation. The comparison results are shown in Table 1.

4.2 Milling force prediction experiments

In order to verify the accuracy of the milling force prediction model of the ball end mill established in this paper, the five-axis milling experiments of complex sculptured surface with arbitrary feeding direction were arranged. The geometrical dimension of the workpiece is shown in Fig. 12 and the

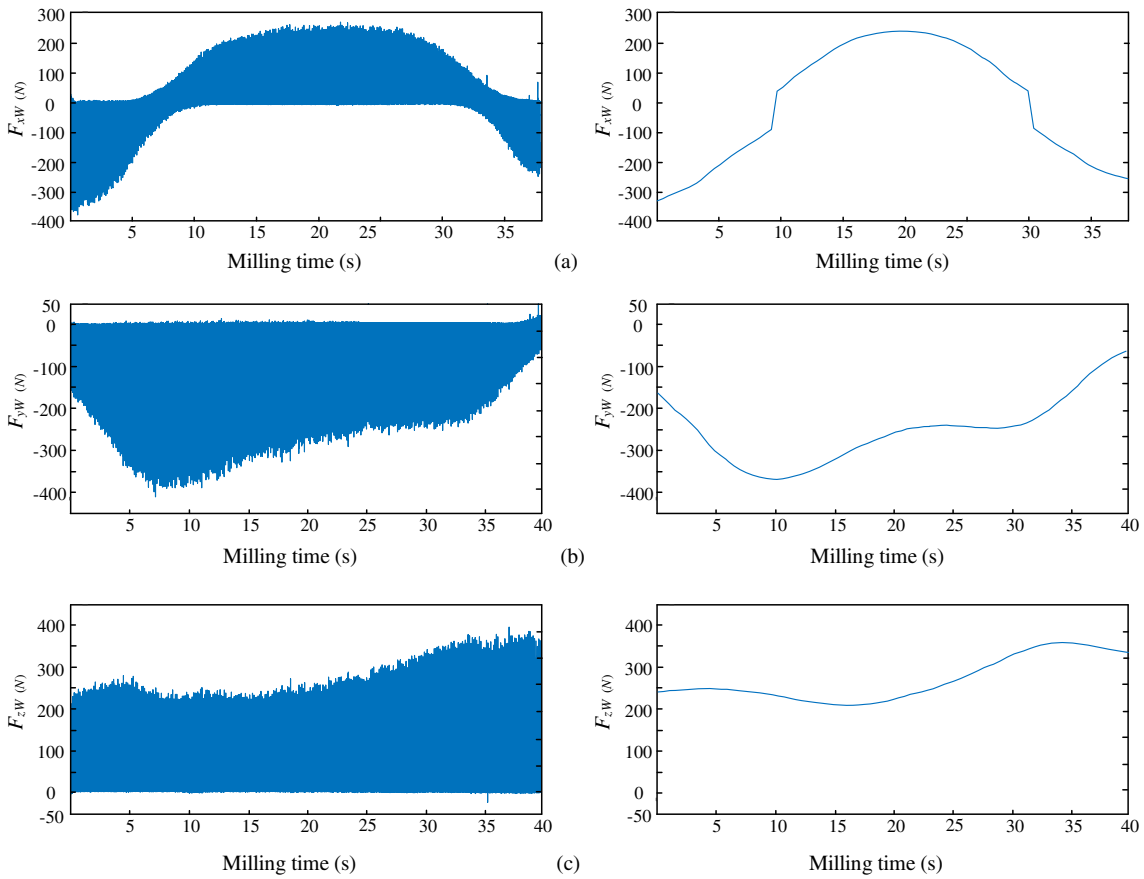

Fig. 16 **a**–**c** Three-direction milling forces predictive results of sinusoidal tool path

material is 45 steel. The designed complex surface equation is $z = 0.0025x^2 + 0.0001307y^{2.8},\ 20 \le x \le 100,\ 20 \le y \le 80$, where Fig. 12a is tool path planning mode with Z-constant and surface workpiece, while Fig. 12b is tool path planning mode with sinusoidal wave and surface workpiece. The reference equation of sinusoidal wave is $y = -20\sin(180x/\pi),\ 0 \le x \le 2\pi$. A Mitsubishi's MIRACLE-coated solid carbide ball end mill with two flutes was used to cut. The diameter of cutter and nominal helix angle are 10 mm and 30°, respectively. The spindle speed, the feed speed, the normal cutting depth, the step distance, and the angle between cutter shaft and the normal of workpiece are 500 r/min, 150 mm/min, 1 mm, 1 mm, and 15°, respectively. The experiments were completed in DMU 60 monoBLOCK five-axis CNC machining center. The force signal was collected by YDX-III9702 three-way piezoelectric milling force measurement platform. The sampling frequency is 5120 Hz and the experimental processing is shown in Fig. 13.

Cutting force coefficients in experiments are as follows:

$$\begin{cases} K_{tc} = 2592k^3 + 20531.3k^2 - 34362.2k + 10955.7 \\ K_{rc} = 167679.7k^3 - 278941.6k^2 + 138272.7k - 19316 \\ K_{ac} = -6167.6k^3 + 2805.3k^2 + 2865.2k - 1849 \end{cases}$$
$$K_{te} = -74.5\ N/mm, K_{re} = -81.2\ N/mm, K_{ae} = -3.8\ N/mm.$$

The coefficients brought into the milling force prediction model established in this paper; the five-axis machining milling force of oblique plane corresponding to the above parameters can be obtained. Figure 14 shows the comparison result of predictive milling force and measured force. The peak and trend of the predictive milling force are in good agreement with measured force, indicating the reliability of the coefficients.

The number of cutter location points of Z-constant tool path machining and sinusoidal tool path machining is 59 and 67 respectively. Each cutter location point can be seen as a five-axis machining of oblique plane. The vector from a cutter location point to next one is feed direction. X_c-axis of cutter coordinate system is the cross product of cutter axis vector and normal direction. Y_c-axis is obtained through right-hand coordinate principle. Combined with milling force predictive model of five-axis ball end milling in the last section, the three-direction milling forces of the two paths mode are shown in Figs. 15 and 16. It shows that a slight deviation in amplitude in Fig. 15c and it shows a slight deviation in the trend of the portion where the milling force is greater than zero Fig. 16a. The errors of predictive force are less than 10%. The possible reason is the local radius of the tool path is small, which results in the larger deviation of the ICCE and the prediction error of the milling force. In general, considering the tool setting error, the machining error, and the location error between the measured force coordinate system and the programming coordinate system, the results of the five-axis machining predictive milling force are in good agreement with the measured results. Also, shorter step length can further reduce the prediction error. The experiments prove the effectiveness of the milling force predictive model of five-axis ball end milling of sculptured surface.

5 Conclusions

Based on space region limitation, this paper proposes the conditions of micro-cutting edge involved in cutting for three-axis ball end milling of horizontal plane. Then, the conditions of micro-cutting edge involved in cutting for five-axis ball end milling of oblique plane can also be achieved based on space rotation transformation. The ICCE is obtained by searching the whole cutting edge. Combining differential discretization thought, the analytical ICCE algorithm of five-axis ball end milling of sculptured surface is presented.

Based on the above-mentioned five-axis ICCE algorithm, combined with micro-element cutting force model and the non-deformed chip thickness model with arbitrary feed direction and cutter axis vector which is suitable for five-axis ball end milling, the milling force predictive model for five-axis ball end milling of sculptured surface is established.

The simulation results of ICCE of three-axis milling of oblique plane and five-axis milling of sculptured surface about ball end mill show that the analytical method has higher accuracy than Z-map method and higher efficiency than solid modeling method. The errors of analytical method are less than 1%. The results of five-axis ball end milling of sculptured surface with Z-constant tool path and sinusoidal tool path show that the predictive milling forces and measured results are well matched in amplitude and trend, which proves the effectiveness of predictive milling force model established in this paper.

Funding information This research is supported by the Natural Science Foundation of Liaoning No. 201602174 and the Fundamental Research Funds for the Central Universities No. DUT17GF213.

References

1. Martellotti ME (1941) An analysis of the milling process. ASME J Manuf Sci Eng 63:677–700
2. Koenigsberger F, Sabberwal AJP (1961) An investigation into the cutting force pulsation during milling operations. Int J Mach Tool Manu 1(1–2):15–33
3. Tlusty J, MacNeil P (1975) Dynamics of cutting forces in end milling. CIRP Ann 24:21–25
4. Kline WA, DeVor RE, Lindberg JR (1982) The prediction of cutting forces in end milling with application to cornering cuts. Int J Mach Tool Manu 22:7–22

5. Yang MY, Park H (1991) The prediction of cutting force in ball-end milling. Int J Mach Tool Manu 31(1):45–54
6. Yucesan G, Altintas Y (1996) Prediction of ball end milling forces. J Eng Ind 118(1):95–103
7. Wang JJJ, Huang CY (2004) A force-model-based approach to estimating cutter axis offset in ball end milling. Int J Adv Manuf Technol 24(11–12):910–918
8. Tsai CL, Liao YS (2010) Cutting force prediction in ball-end milling with inclined feed by means of geometrical analysis. Int J Adv Manuf Technol 46:529–541
9. Azeem A, Feng HY (2013) Cutting force prediction for ball-end mills with non-horizontal and rotational cutting motions. Int J Adv Manuf Technol 67(5–8):1833–1845
10. Imania BM, Sadeghib MH, Elbestawi MA (1998) An improved process simulation system for ball-end milling of sculptured surfaces. Int J Mach Tool Manu 38(9):1089–1107
11. Guzel BU, Lazoglu I (2004) An enhanced force model for sculptured surface machining. Mach Sci Technol 8(3):431–448
12. Sun YW, Ren F, Guo DM, Jia ZY (2009) Estimation and experimental validation of cutting forces in ball-end milling of sculptured surfaces. Int J Mach Tool Manu 49(15):1238–1244
13. Wei ZC, Wang MJ, Cao YJ, Wang SF (2013) Prediction of cutting force in ball-end milling of sculptured surface using improved Z-map. Int J Adv Manuf Technol 51(5):428–432
14. Jia ZY, Ge J, Ma JW, Gao YY, Liu Z (2016) A new cutting force prediction method in ball-end milling based on material properties for difficult-to-machine materials. Int J Adv Manuf Technol 86: 2807–2822
15. Fontaine M, Devillez A, Moufki A, Dudzinski D (2006) Predictive force model for ball-end milling and experimental validation with a wavelike form machining test. Int J Mach Tool Manu 46(3):367–380
16. Ozturk E, Budak E (2005) Modeling of 5-axis milling forces. Proceedings of the 8th CIRP International Workshop Model Machining Operations, May 10–11, Chemnitz, Germany, 319–332
17. Ozturk E, Budak E (2007) Modeling of 5-axis milling processes. Mach Sci Technol 11(3):287–311
18. Boz Y, Erdim H, Lazoglu I (2011) Modeling cutting forces for 5-axis machining of sculptured surfaces. Adv Mater Res 223:701–712
19. Yang Y, Zhang WH, Wan M, Ma YC (2013) A solid trimming method to extra cutter-workpiece engagement maps for multi-axis milling. Int J Adv Manuf Technol 68(9–12):2801–2813
20. Zhu RX, Kapoor SG, DeVor RE (2001) Mechanistic modeling of the ball end milling process for multi-axis machining of free-form surfaces. J Manuf Sci Eng 123(3):369–379
21. Fussell BK, Jerard RB, Hemmett JG (2003) Modeling of cutting geometry and forces for 5-axis sculptured surface machining. Comput Aided Des 35(4):333–346
22. Guo DM, Ren F, Sun YW (2010) An approach to modeling cutting forces in five-Axis ball-End milling of curved geometries Based on tool motion analysis. J Manuf Sci Eng 132(4):575–590
23. Wang SB, Geng L, Zhang YF, Liu K, Ng TE (2015) Cutting force prediction for five-axis ball-end milling considering cutter vibrations and run-out. Int J Mech Sci 96–97:206–215
24. Geng L, Liu PL, Liu K (2015) Optimization of cutter posture based on cutting force prediction for five-axis machining with ball-end cutters. Int J Adv Manuf Technol 78(5–8):1289–1303
25. Sun Y, Guo Q (2011) Numerical simulation and prediction of cutting forces in five-axis milling processes with cutter run-out. Int J Mach Tool Manu 51(10):806–815
26. Huang T, Zhang X, Ding H (2013) Decoupled chip thickness calculation model for cutting force prediction in five-axis ball-end milling. Int J Adv Manuf Technol 69(5–8):1203–1121